

Treatment of Petroleum Refinery Wastewater by Electrooxidation Using Anode Composed of Composite Materials

Mohammed Hammid Jaesh

University of Al-Qadisiyah

Husham M. Al-Tameemi

University of Al-Qadisiyah

Abstract: Wastewater discharged from an Iraqi petroleum refinery plant was treated in the current work utilizing an electrooxidation method made up of anodic oxidation employing an aluminum and graphite (Al-Gr) composite anode. The effectiveness of the anodic oxidation process was assessed by applying the response surface methodology (RSM-CCD) and using a batch-recirculation mode. Three key operating parameters were taken into account: time (30-120), pH (3-9), and current density (4-12 mA/cm²). The COD value decreased well, according to the results. A current density of 12 mA/cm², a pH of 3, and an operating duration of 120 minutes were the ideal working parameters, resulting in a RE% of 96.1%. ANOVA results showed that the current density, with a 45.98% contribution, had the biggest impact on RE%, followed by time and pH. The anodic process demonstrated that it was possible to obtain greater removal efficiency while using less energy, highlighting the significance of applying electrochemical processes as alternative, environmentally friendly, and economically viable wastewater treatment methods.

Keywords: Aluminum, Anodic oxidation, Composite materials, Graphite, Petroleum refinery wastewater

Introduction

One of the natural resources that is vital to human activity and the evolution of life is water. It is essential for nations to thrive and flourish as well as for providing clean water, which is essential for human consumption (Al-Malack & Siddiqui, 2013). The increasing need for energy worldwide, which is expected to increase by 44% over the next few decades, prompted experts to look into more effective methods of treating oily wastewater (Husin et al., 2011; Newell et al., 2016). The petroleum refinery sector uses a variety of refinery operations, such as distillation, hydrocracking, desalination systems, and cooling units, to produce over 2500 important goods. Kerosene, diesel fuel, liquefied petroleum gas, lubricating oils, gasoline, aviation fuel, and fuel oils are a few examples of these items (Yu et al., 2014). A significant amount of fresh water was used in the associated refinery processes as a result of producing these enormous quantities of products, which resulted in the production of a significant amount of wastewater (Yu et al., 2014). This wastewater's high salinity and chemical oxygen demand (COD) make it a crucial source of environmental contamination. Because it contains a lot of hazardous substances, it needs to be effectively treated before being released into the environment (Alva-Argáez et al., 2007; Smith, 1998).

The amount of wastewater produced by refining processes is about 1.6 times that of the processed crude oil, with 80-90% of that amount ending up as wastewater. Therefore, treating these wastewaters can benefit refinery plants financially by allowing them to reuse treated water and lowering pollution (Diya'uddeen et al., 2011; Mota, 2005). A refinery plant's wastewater sent to the treatment unit would be tainted with a variety of dangerous compounds, including light fraction aliphatic, chlorinated organics, and aromatic petroleum

- This is an Open Access article distributed under the terms of the Creative Commons Attribution-Noncommercial 4.0 Unported License, permitting all non-commercial use, distribution, and reproduction in any medium, provided the original work is properly cited.

- Selection and peer-review under responsibility of the Organizing Committee of the Conference

hydrocarbons. Therefore, using cost-effective and active techniques to treat these wastewaters is essential (Aljuboury et al., 2017).

Mechanical and physicochemical techniques like gravity separation and skimming, coagulation, de-emulsification, air flotation, and flocculation followed by biological treatment are among the traditional treatment methods used for wastewater discharged from refineries (Stepnowski et al., 2002). These conventional techniques have numerous disadvantages, including high operating costs, poor efficiency, corrosion issues, producing large amounts of sludge, and producing large amounts of secondary pollutants, like sulfate and chloride, through coagulation and precipitation (Abdeen, 2019; Akyol, 2012; Moussavi et al., 2011).

The use of electrochemical techniques for wastewater treatment has garnered a lot of attention in the last ten years because of their many unique advantages, which include adaptability, safety, energy efficiency, selectivity, and automation compatibility (Alattar et al., 2023; Khaleel et al., 2023; Martínez-Huitle & Brillas, 2009; Salman & Abbar, 2023; Yavuz et al., 2010). One kind of electrochemical technique that is much sought after for treating wastewater from petroleum refineries at a low cost and high removal effectiveness is electrooxidation (Fu et al., 2023).

This process typically reduces the pollutants in wastewater by mineralizing them as a result of the system's production of free radicals. Direct and indirect processes are two categories for electro-oxidation operation methods (Al-Ameri et al., 2023; Asfaha et al., 2021; Hoang et al., 2021; Sundaramoorthy et al., 2023). Direct electron movement causes the polluting materials to undergo an oxidizing reaction at the anode electrode during the direct oxidation process. However, the electrolytic reaction mechanism that works on contaminants in the indirect oxidation process produces active species such chlorine, iron salts, Ag, Ni, Ce, and Co ions. Because these active organisms produce a secondary pollution in the system, their usage is typically limited (Fu et al., 2023).

The electrooxidation process's mechanism is influenced by a number of variables, such as the type of electrode, the concentration of pollutants, the pH level, and the applied operating voltage. To produce efficient hydroxyl radical oxidants, anodes are typically employed in the direct oxidation method (Abbar & Alkurdi, 2021; Ansari & Nematollahi, 2018; Itoi et al., 2023; Jiang et al., 2021; Machado et al., 2018; Mandal et al., 2017; Martínez-Huitle & Panizza, 2018; Peng et al., 2020; Shao et al., 2020). Tin oxide has been successfully used as an anodic material in Li-ion batteries (Chang et al., 2004) as well as other applications such as solar cells (Ayllon & Lira-Cantu, 2009), catalysts (Kowal et al., 2009), and gas sensors (Zhang et al., 2009). To anodically oxidize a range of wastewater types and organic compounds, such as textile, landfill leachate, phenol, nitrophenols, and glucose, several SnO₂-based anodes have been used in wastewater application (Ho et al., 2022).

The objective of this work is to investigate the feasibility of anodic oxidation using an Al:Gr anode in an electrooxidation flow system that runs at batch circulation with the proper electrochemical reactor architecture. RSM was used to investigate how operational parameters such as time, pH, and current density (C.D.) affected the recovery of COD from wastewater generated by the Al-Diwaniyah petroleum refinery. Since circulation improves mass transfer and is therefore one of the main elements influencing the removal process, the current work's adoption of the batch-recirculation mode is based on its successful application in treating a range of wastewaters.

Furthermore, it is easy to scale up this configuration (Khataee et al., 2013; Khataee et al., 2014). An experimental design was selected for this task since the conventional approach (one component at a time) is unable to determine the effects of interaction among the factors that could be advantageous on the process's efficiency. Furthermore, RSM can be used to reduce the number of runs, the expense, and the amount of time required to finish the tests (Alizadeh et al., 2022; Jiad & Abbar, 2023).

Materials and Methods

Characteristics of Petroleum Refinery Effluents

Forty liters of wastewater from the Al-Dewaniyah refinery facility in Iraq were collected from the feeder collecting tank of the biological treatment unit and kept at 4°C until they were needed for this experiment. Prior to any runs, a filtration step was carried out using a vacuum pump and Puchner and Whatman filter paper Grade 1 (medium flow filter paper) with a particle size of 11 µm in order to lessen the turbidity of the wastewater

sample. Based on the biological unit supplied by the plant administration, Table 1 shows the properties of both treated and untreated wastewater.

Table 1. Characteristics of Al-Dewaniyah refinery plant wastewater

pH	Temperature °C	TDS ppm	BOD ppm	COD ppm	Phenol ppm	Oil Mg/l	Turbidity NTU	PO ₄ ³⁻ ppm	Cl ⁻ ppm
7.2	20	4200		850		21.25	113	0.55	600

Chemicals

A range of materials were used in this investigation, including composites of graphite and aluminum for the anode electrode and local stainless steel for the cathode electrode. The chemicals H₂SO₄ (made in FINE CHEM LIMITD, INDIA) and NaOH (manufactured in BDH Chemicals Ltd pool, England) are also used to neutralize (pH) wastewater from oil refineries. To improve the solution's conductivity, sodium chloride (NaCl), which is made locally (99.5%, THOMAS BAKER, India), was also added, as well as utilizing distilled water to clean the experiment's equipment (0.5-3 Ms/cm).

The Electrochemical System

Figure 1 provides a conceptual and graphic representation of the electrochemical system. The electrochemical system was made up of a tubular-designed electrochemical reactor that was utilized in batch-recycling mode, as seen in Figure 1. With an external diameter of 130 mm and a thickness of 10 mm, the cell body and cover were made of Perspex. The size of the electrochemical cell is 90 × 130 mm. The lateral surface of the cell body has an entrance with a diameter of 5 mm. The body was fastened to the cover by joining the body cell at the top with a four-holed flange.

The lid had two holes: a 40 mm diameter hole 40 mm from the center that served as an exit, and a 10 mm diameter hole in the middle that held the anode in place. Four bolts and nuts can be used to secure the cover's four holes to the cell body. The electrochemical reactor structure used in this work is based on a concentric electrode layout. The cathode was a hollow 316L stainless steel cylinder. Its dimensions are 70 mm for the outer diameter and 80 mm for the length. A bolt and nut were positioned in the center of its length to secure it inside the cell body.

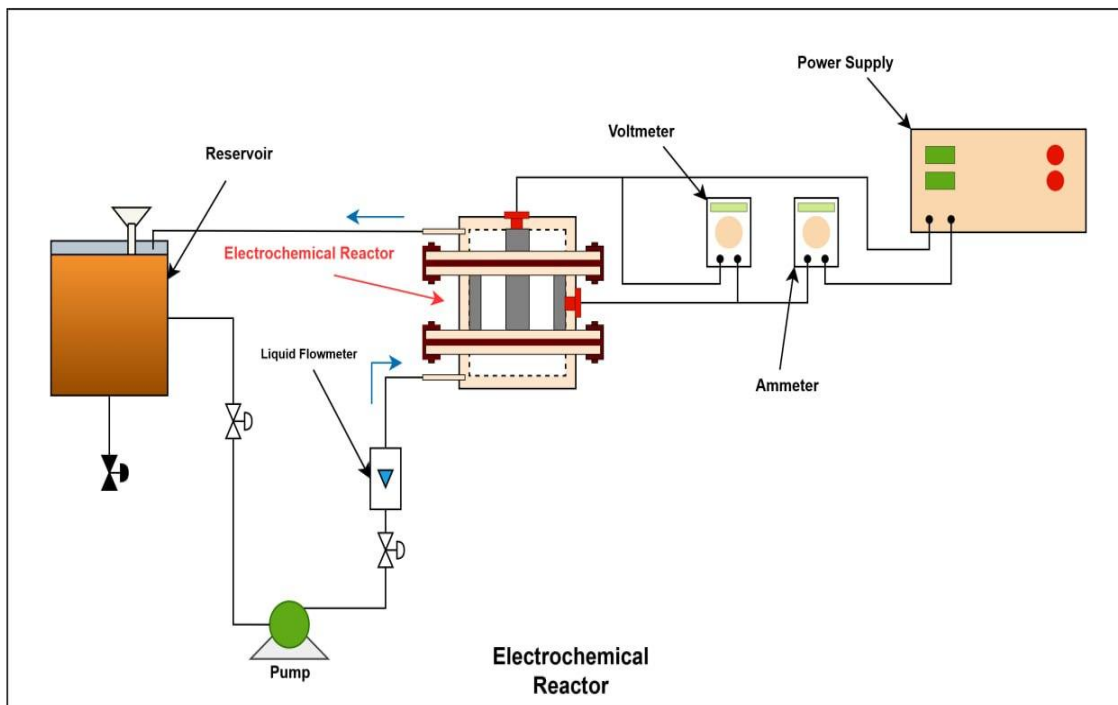


Figure 1. Configuration of electrooxidation system

The anode was created using a graphite and aluminum combination. An adequate current density was applied across the electrodes using a digital power source. It was a 1.5-liter glass tank that was 150 mm by 110 mm and had a matching Perspex top. The treated water is discharged from the first exit, which is 10 mm in diameter and situated at the bottom. The second exit, which is also 10 mm in diameter and situated at the lateral surface of the electrochemical cell, is then used to transfer the cleaned water using a recirculation pump. The tank lid was 140 mm in diameter and 10 mm thick, with two perforations. One to provide the midway response.

The last one is used to inject air from an air compressor, while the second one, which has a diameter of 10 mm, is used to collect effluent from the electrochemical reactor. The wastewater flow rate was set at 4 L/min using a flow meter. The anode was created using a graphite and aluminum combination. An adequate current density was applied across the electrodes using a digital power source. It was a 1.5-liter glass tank that was 150 mm by 110 mm and had a matching Perspex top. The treated water is discharged from the first exit, which is 10 mm in diameter and situated at the bottom. The second exit, which is also 10 mm in diameter and situated at the lateral surface of the electrochemical cell, is then used to transfer the cleaned water using a recirculation pump. The tank lid, which was 140 mm in diameter and 10 mm thick, featured two apertures, one in the center of which provided the response. The last one is used to inject air from an air compressor, while the second one, which has a diameter of 10 mm, is used to collect effluent from the electrochemical reactor. The wastewater flow rate was set at 4 L/min using a flow meter.

Analytical Measurements

The COD test is a widely used and reliable method for determining the organic content of wastewater. By determining the total amount of oxygen needed to transform organic molecules into carbon dioxide and water, the test enables waste assessment. This study used COD as a responder to evaluate the viability of the electrooxidation process for the degradation of organic contaminants in petroleum refinery effluent. K₂Cr₂O₇ was used as an oxidizing agent in a thermal reactor (RD125, Lovibond) to digest 2 cc of effluent for 120 minutes at 150 °C in order to determine the COD.

Performance Evaluation

COD removal efficiency was calculated by the following equation (Jiad & Abbar, 2023):

$$RE\% = \frac{COD_i - COD_f}{COD_i} \times 100 \quad (1)$$

Where $RE\%$ means COD removal efficiency, the initial value of COD in (mg/L) denotes by COD_i while final value of COD in (mg/L) terms as COD_f .

Electrical energy consumption is an essential economic parameter in the electrooxidation process. In this work, electrical energy consumption in electrooxidation process (EEC) was calculated using the following equation (Jiad & Abbar, 2023):

$$EEC = \frac{U \cdot I \cdot t}{V} \quad (2)$$

Where EEC is the EO electrical energy in kWh/m³, I denotes the current in ampere (A) and U denotes the cell voltage in volt (V).

Experimental Design

A group of statistical and mathematical techniques known as response surface methodology (RSM) are used to optimize the response's operational circumstances, which are impacted by a number of process operating variables. One of the best designs utilized in RSM to validate and test the process parameters that affected the removal of COD was the Box-Behnken design (CCD), which has four components and three levels.

Four process variables - C.D. (X1), pH (X2), and time (X3) - were regarded as process factors in the CCD. Their coded levels were -1 (low level), 0 (middle level), and +1 (high level), and RE% was regarded as a response (El-Ghenemy et al., 2012). The process variables and their selected levels are shown in Table 2.

Table 2. Process parameters in the refinery wastewater treatment (coded levels)

Process parameters Coded levels	Range in central composite				
	Low (α)	Low (-1)	Middle (0)	High (+1)	High (α)
X1 current density (mA/cm ²)	2	4	7	10	12
X2: pH	3	4	6	8	9
X3: Time (min)	20	40	70	100	120

Using a subset of the chosen runs for a three-level factorial, Box-Behnken provides the designs needed to create the proper quadratic model with the acceptable statistical criteria. The number of runs (N) needed to finish a Box-Behnken design can be estimated using the following formula (El-Ghenemy et al., 2012):

$$N = 2k(k-1) + cp \quad (3)$$

Where variables number is represented by k and number of repeating the central point by cp .

Based on Equation (3), 27 runs should be performed to identify the interactions among variables and their impact on the RE%. Table 4 displays the BBD array proposed for this study.

A second order polynomial model could be formulated based on CCD as shown in the following equation:

$$Y = a_0 + \sum a_i x_i + \sum a_{ii} x_i^2 + \sum a_{ij} x_i x_j \quad (4)$$

According to Equation (4), the COD removal could be represented as a response Y and x_1, x_2, \dots, x_k represent the process factors. a_0 is intercept term, i and j denotes the index numbers for patterns, a_i denotes the 1st.order main effect, a_{ii} symbolizes the 2nd. order main effect, and a_{ij} acts the impact of interactions. After the illative analysis, a regression coefficient (R^2) is estimated for checking the fitting of model.

Table 3. Experimental design by central composite design (CCD) of electrooxidation process

Run Order	Pt Type	Blocks	Current density (mA/cm ²)	pH	Time(min)
1	1	1	4	4	40
2	1	1	10	4	40
3	1	1	4	8	40
4	1	1	10	8	40
5	1	1	4	4	100
6	1	1	10	4	100
7	1	1	4	8	100
8	1	1	10	8	100
9	-1	1	2	6	70
10	-1	1	12	6	70
11	-1	1	7	3	70
12	-1	1	7	9	70
13	-1	1	7	6	20
14	-1	1	7	6	120
15	0	1	7	6	70
16	0	1	7	6	70
17	0	1	7	6	70
18	0	1	7	6	70
19	0	1	7	6	70
20	0	1	7	6	70

Table 4. Results of COD removal by electrooxidation process (AC/3Al: 3Gr)

Run Order	Pt Type	Current density (mA/cm ²)	pH	Time (min)	RE%	COD _f	EEC _T (kWh/m ³)
1	1	4	4	40	136	84	0.60496
2	1	10	4	40	68	92	1.37310
3	1	4	8	40	127.5	85	0.59700
4	1	10	8	40	93.5	89	1.44076
5	1	4	4	100	76.5	91	1.39300
6	1	10	4	100	34	96	3.58200
7	1	4	8	100	93.5	89	1.42484
8	1	10	8	100	59.5	93	3.52230
9	-1	2	6	70	110.5	87	0.45969
10	-1	12	6	70	34	96	5.18196
11	-1	7	3	70	76.5	91	2.07209
12	-1	7	9	70	110.5	87	2.09647
13	-1	7	6	20	110.5	87	0.54327
14	-1	7	6	120	51	94	3.51036
15	0	7	6	70	85	90	2.02333
16	0	7	6	70	76.5	91	1.99896
17	0	7	6	70	85	90	2.05746
18	0	7	6	70	76.5	91	1.99896
19	0	7	6	70	76.5	91	2.01358
20	0	7	6	70	85	90	1.99896

Minitab-19 software was used in this analysis and then a quadratic model was developed in terms of the real values of the system factors which relate the RE% to the process factors as shown in the following equation:

$$RE\% = 67.48 + 1.345X_1 - 2.9437X_2 + 0.1524X_3 + 0.0326X_1 \cdot X_1 - 0.1913X_2 \cdot X_2 - 0.00004X_3 \cdot X_3 + 0.1042X_1 \cdot X_2 + 0.00417X_1 \cdot X_3 + 0.00625X_2 \cdot X_3 \quad (5)$$

Where X_1, X_2, X_3 acts process factors while X_1X_2, X_1X_3 and X_2X_3 denote to the interaction influence among these variables. X_1^2, X_2^2, X_3^2 represent a measure of the double influence of these variables. Synergistic as well as antagonistic effects are denoted by (+, -) signs in front of each parameter as well as their interaction terms (Kalantary et al., 2018).

Table 5 displays the model's ANOVA findings, where DF denotes degree of freedom and Seq. SS Adj. SS and Adj. MS stand for sum of the square, adjusted sum of the square, and adjusted mean of the square, respectively, whilst (Contr. %) indicates the contribution of each factor. Fishermen: The model's ability was evaluated using the F-test and P-test; a high Fisher value suggests that the regression equation may be applied to fit the maximum diversity bounds. To ascertain whether the F-value is high enough to identify the statistical significance of the model, the P-value is employed.

If the P-value is less than 5%, 95% of the model's chargeables may be taken into account (Ghasempur et al., 2007). According to Table 5's findings, the quadratic model is significant with a P-value of 0.0003 and an F-value of 22.51. The lack of fit test may be used to ensure that the selected model is sufficient for describing the data or more the conditions required for a complex model (Liu & Chiou, 2005). Comparing lack of fit to pure error in the current investigation, the P-value was $0.647 > 0.05$, indicating that it was not statistically significant (Liu & Chiou, 2005). Consequently, the model is able to match the response values and generate precise predictions. The study found that the experimental data and the expected model values were consistent, with R^2 and adj. R^2 values of 0.9806 and 0.9632, respectively (Liu & Chiou, 2005).

Time (X1) has the biggest importance parameter determining RE%, at 48.89%, according to Table 5, which illustrates the contribution of current density to the breakdown of organic pollutants during electro oxidation. With 35.54% of the total, time is the second element that affects the removal of COD. 6.93 percent was the least significant characteristic affecting RE% as a percentage of contribution. This suggests that time and current density have a major impact on the process. Furthermore, all 2-way interactions are non-significant, and the contribution of the 2-way interaction has an effect of 2.75% on the RE% that may be disregarded (Jiad & Abbar, 2024). Quadratic interactions had a large impact on the RE%, which helped 3.68%.

Table 5. ANOVA results of COD removal by electrooxidation process (AC/3Al: 3Gr)

Source	DF	Seq. SS	Contr.%	Adj. SS	Adj. MS	F-value	P-value
Model	9	191.420	98.06%	191.420	21.2689	56.27	0.000
Linear	3	178.504	91.45%	178.504	59.5012	157.43	0.000
X1	1	95.607	48.98%	95.607	95.6066	252.96	0.000
X2	1	13.520	6.93%	13.520	13.5200	35.77	0.000
X3	1	69.377	35.54%	69.377	69.3770	183.56	0.000
Square	3	7.542	3.86%	7.542	2.5139	6.65	0.010
X1*X1	1	1.500	0.77%	1.217	1.2170	3.22	0.103
X2*X2	1	5.980	3.06%	6.021	6.0207	15.93	0.003
X3*X3	1	0.062	0.03%	0.062	0.0623	0.16	0.693
2-Way Inter.	3	5.375	2.75%	5.375	1.7917	4.74	0.026
X1*X2	1	3.125	1.60%	3.125	3.1250	8.27	0.017
X1*X3	1	1.125	0.58%	1.125	1.1250	2.98	0.115
X2*X3	1	1.125	0.58%	1.125	1.1250	2.98	0.115
Error	10	3.780	1.94%	3.780	0.3780		
Lack of fit	5	2.280	1.17%	2.280	0.4559	1.52	0.329
Pure-Error	5	1.500	0.77%	1.500	0.3000		0.000
Total	19	195.200	100.00%				0.000
Model Summary		S	R ²	R ² (adj.)	Press	R ² (pred.)	
		0.614781	98.06%	96.32%	21.6391	88.91%	

Effect of Operating Parameters

To determine the effect of process elements and their interactions on RE%, graphic plots of the quadratic model were created. The combined effects of current density and pH on the RE% at 70-minute intermediate time periods are shown in Figure 2. The response surface is depicted in Figure 2 (a), and the corresponding contour plot is shown in Figure 2 (b). Figure 3 (a) illustrates how the RE% increases in tandem with the current density. At low pH levels, the connection appears to be linear, but at high catalyst concentrations, it tends to be exponential. This pattern implies that the current density is the main factor influencing electron mobility and the generation of reactive oxidants (Baddouh et al., 2019; Molla Mahmoudi et al., 2022), which in turn affects the rates at which pollutants are removed.

Numerous studies have indicated that current densities have a substantial impact on the removal of pollutants from different wastes (Jawad & Abbar, 2019; Morales et al., 2018; Peralta-Hernández et al., 2016; Santos et al., 2013). When it comes to pH effects, things are different. When the system was operating at high current density, it was found that raising the pH value decreased removal efficiency. However, it also decreased removal rate until it began to increase. The results of this investigation (Figure 2 (b)) suggest that a pH range of 5-7 and a current density of 10-12 mA/cm² could result in R.E% > 95%.

Figure 3 shows how the RE% at intermediate pH levels is influenced by both duration and current density. The response surface plot is shown in Figure 3 (a), and the corresponding contour plot is shown in Figure 3 (b). It is evident from Figure 3 (a) that the RE% of pollution clearance rises with time and current density. Even though duration has less of an impact than current density, RE% increased dramatically with increasing time, as shown in Table 5. Since the oxidation reaction takes longer to oxidize the organic pollutants, it has been claimed that the efficiency of electrooxidation in removing contaminants peaks at particular ideal times.

It was clear from the contour plot results (Figure 2 (b)) that an area with a duration of 60 to 80 and a current density of 11 to 12 mA/cm² could have R.E% > 95 %. Figure 4 illustrates the whole effects of pH and time on the RE% with a current density of 7. Figure 4 (a) displays the response surface plot, whereas Figure 4 (b) displays the matching contour plot. The RE% grew linearly when the pH value was elevated to 6, and it began to fall after pH = 6, as shown in Figure 2 (a). Furthermore, the relationship between increasing time and increasing RE% is almost linear. Table 5 shows that time has a more pronounced effect than pH. The fact that more hydroxyl radicals are created over time to complete the oxidation reactions that oxidize the organic molecules may help to explain this phenomenon. The contour plot results (Figure 4 (b)) clearly show that R.E% > 90% may be reached in a specific region where the pH is between 90 and 120 minutes and the time is within 3-6.5.

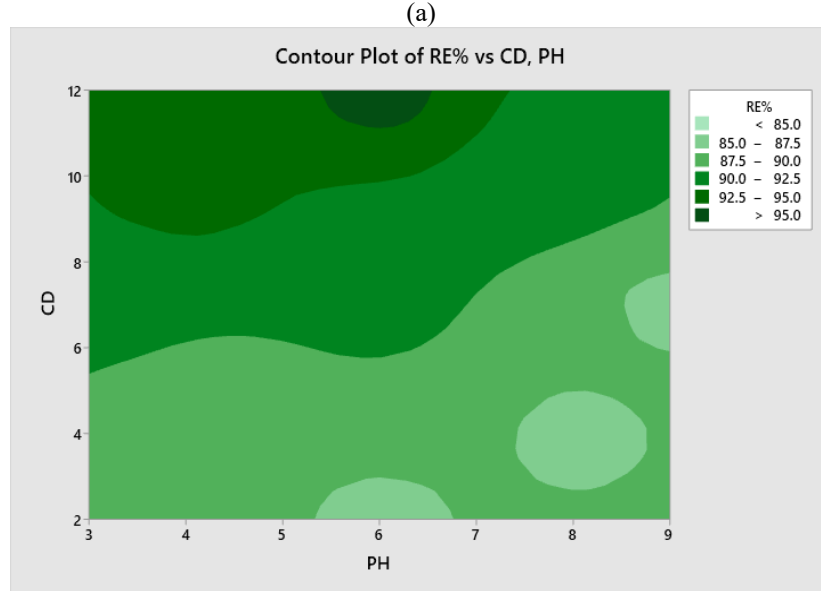
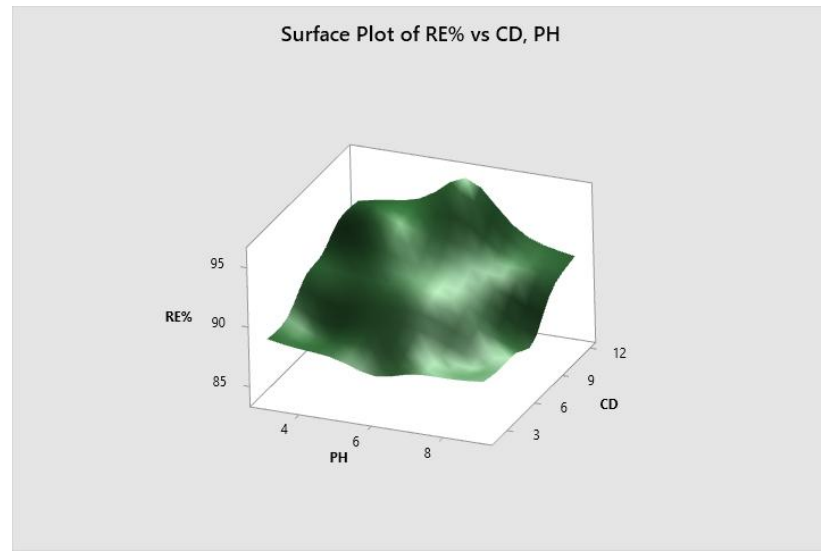
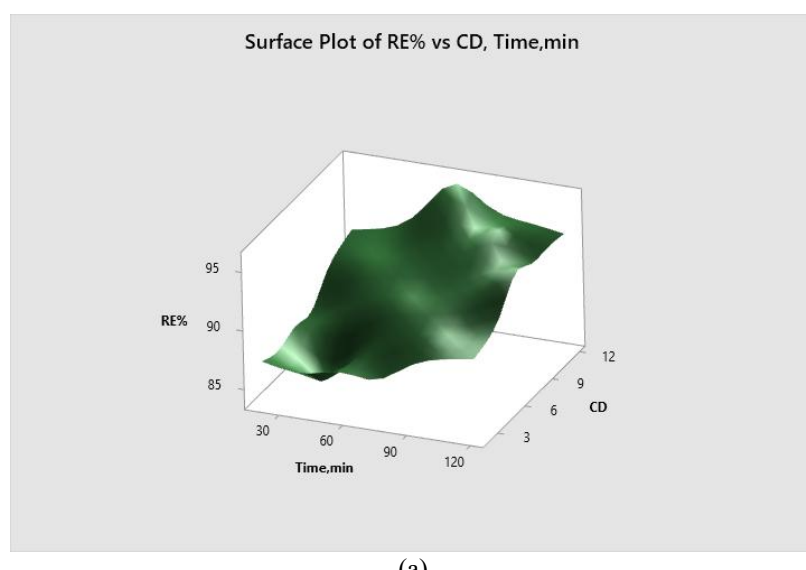
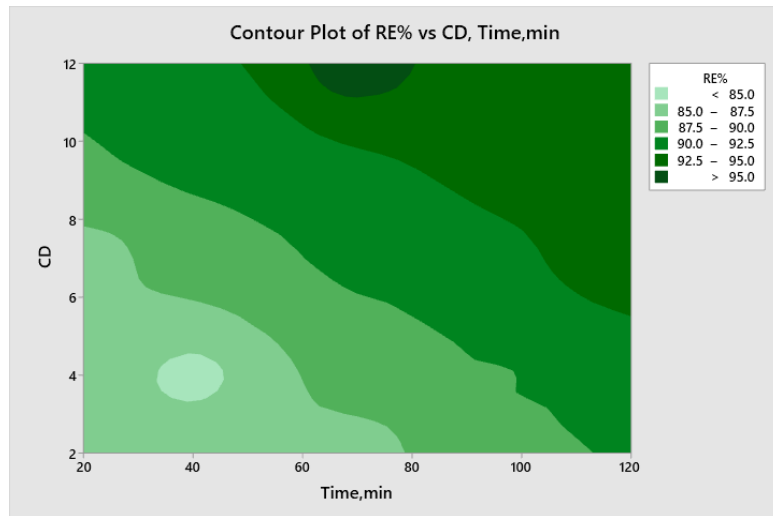


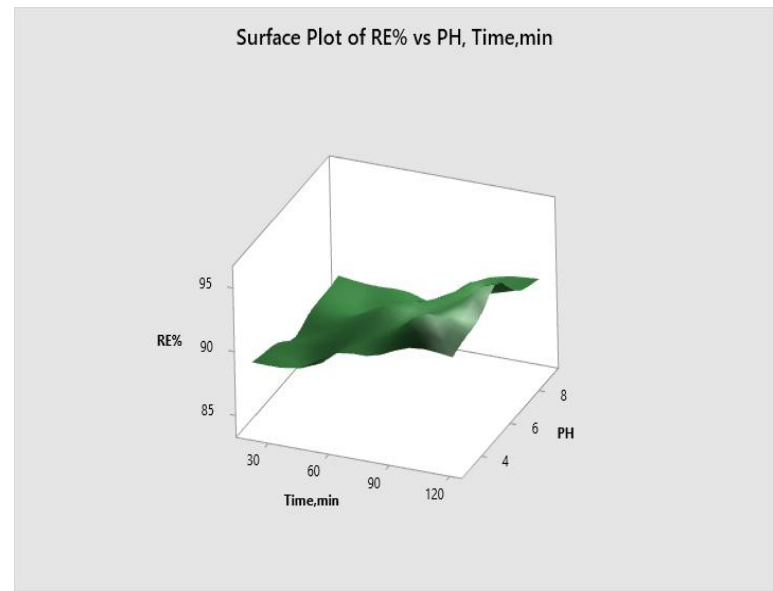
Figure 2. (a) 3D plot of interaction between current density and pH, (b) contour plot between current density and pH



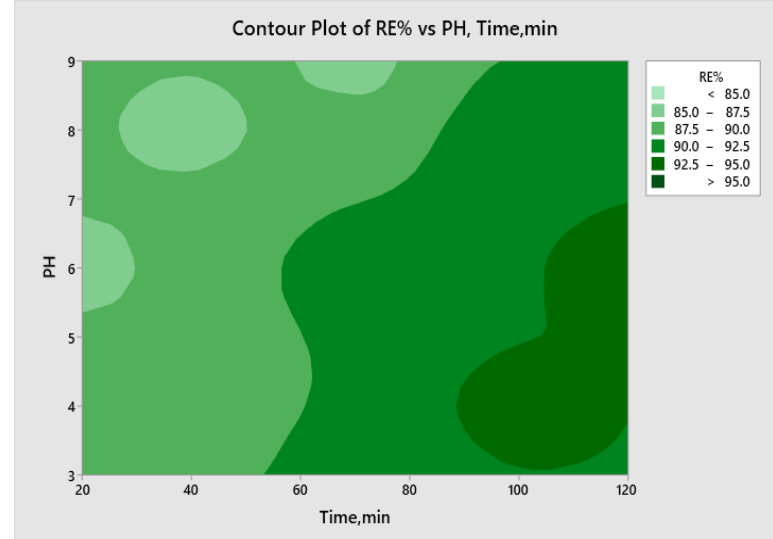


(b)

Figure 3. (a)3D plot of interaction between current density and time, (b) contour plot between current density and time



(a)



(b)

Figure 4 (a) 3D plot of interaction between pH and time, (b) contour plot between pH and time

Optimization

Any optimization process's primary goal is to maximize the response's value. Consequently, with a desire weight of 1.0, RE% was proposed as the upper limit. Minitab-19 software's optimizer has been used to determine optimization. Table 6 provides an explanation of the optimization results, using DF = 1 as the ideal.

Table 6. Response optimization based on RE%

Response	Aimed	Lower	Target	Upper	Weight	Importance
RE (%)	Max.	84.000	Max	96.000	1	1
Results				Parameters		
Current density (mA/cm ²)	pH	Time (min)	RE% Fit	D _f	SE Fit	95% CI
12	3	120	100.648	1	1.25	(97.86,103.44)
						95% PI
						(97.54,103.76)

Under ideal operating conditions, a maximum removal of 84% is achievable, as Table 6 demonstrates. Since it was anticipated that the COD value would exceed the 100-ppm regulation limit, three tests were conducted using the optimum settings listed in Table 7. In addition to the confirmation investigations conducted under ideal circumstances and displayed in Table 6, an average removal efficiency of 96.1% that was close to the ideal theoretical value was attained. This implies that RSM was successful in providing a high level of confidence on the relationship between the variables in the combined process.

Table 7. Confirmative runs for optimum of RE%

Run	Current density (mA/cm ²)	pH	Time (min)	COD _f (ppm)	RE%
1	12	3	120	34	96
2	12	3	120	32.2	96.2

Verification of the Results

As indicated in Table 7, two experiments were carried out utilizing the optimized parameters in order to validate the optimization results. At 120 minutes into the photocatalysis process, the average COD removal efficiency (average value) was 96.1%, falling within the range of the ideal value based on ideal results (Table 6). With Al-Gr as the anode, central composite design with DF can therefore be a helpful technique to maximize the electrooxidation process RE%.

Conclusion

Anodic oxidation's viability for treating effluent from petroleum refineries was successfully investigated. RSM-CCD was used to optimize the effects of three parameters on the RE%: current density, pH, and time. The findings of the ANOVA indicate that the two most important variables influencing the mechanism of the anodic oxidation process are current density and time. However, the pH level affects COD elimination in a secondary way. The following were the optimal circumstances: Time = 120 minutes, pH = 3, and current density = 12 mA/cm². The ideal RE% was 96.1%. The model's 96.32% R² score attests to the effectiveness of RSM in demonstrating the relationship between the response and process variables.

Scientific Ethics Declaration

* The authors declare that the scientific ethical and legal responsibility of this article published in EPSTEM journal belongs to the authors.

Conflict of Interest

* The authors declare that they have no conflicts of interest

Funding

* No funding.

Acknowledgements

* This article was presented as an oral presentation at the International Conference on Engineering and Advanced Technology (ICEAT) held in Selangor, Malaysia, on July 23-24, 2025.

* The authors acknowledge the assistance of chemical engineering department, the University of Al-Qadissiyah.

References

Abbar, A. H., & Alkurdi, S. S. (2021). Performance evaluation of a combined electrocoagulation–electrooxidation process for the treatment of petroleum refinery wastewater. *IOP Conference Series: Materials Science and Engineering*, 1076, 012027.

Abdeen, Z. (2019). Treatment of Oily Wastewater Using Hydrogels. In *Microbial Action on Hydrocarbons* (pp. 527-541). Springer, Singapore.

Akyol, A. (2012). Treatment of paint manufacturing wastewater by electrocoagulation. *Desalination*, 285, 91-99.

Al-Malack, M. H., & Siddiqui, M. (2013). Treatment of synthetic petroleum refinery wastewater in a continuous electro-oxidation process. *Desalination and Water Treatment*, 51(34-36), 6580-6591.

Al-Ameri, W., Elhassan, A., & Maher, R. (2023). Optimization of electro-oxidation and electro-Fenton techniques for the treatment of oilfield produced water. *Water and Environment Journal*, 37(1), 126-141.

Alattar, S. A., Sukkar, K. A., & Alsaffar, M. A. (2023). Enhancement of ozonation reaction for efficient removal of phenol from wastewater using a packed bubble column reactor. *Indonesian Journal of Chemistry*, 23(2), 383-394.

Alizadeh, S., Sadeghi, H., Vosoughi, M., Dargahi, A., & Mokhtari, S. A. (2022). Removal of humic acid from aqueous media using Sono-Persulphate process: optimization and modelling with response surface methodology (RSM). *International Journal of Environmental Analytical Chemistry*, 102(16), 3707-3721.

Aljuboury, D., Palaniandy, P., Abdul Aziz, H., & Feroz, S. (2017). Treatment of petroleum wastewater by conventional and new technologies-A review. *Global NEST Journal*, 19(3), 439-452.

Alva-Argáez, A., Kokossis, A. C., & Smith, R. (2007). The design of water-using systems in petroleum refining using a water-pinch decomposition. *Chemical Engineering Journal*, 128(1), 33-46.

Ansari, A., & Nematollahi, D. (2018). A comprehensive study on the electrocatalytic degradation, electrochemical behavior and degradation mechanism of malachite green using electrodeposited nanostructured β -PbO₂ electrodes. *Water Research*, 144, 462-473.

Asfaha, Y. G., Tekile, A. K., & Zewge, F. (2021). Hybrid process of electrocoagulation and electrooxidation system for wastewater treatment: a review. *Cleaner Engineering and Technology*, 4, 100261.

Ayllon, J. A., & Lira-Cantu, M. (2009). Application of MEH-PPV/SnO₂ bilayer as hybrid solar cell. *Applied Physics A*, 95, 249-255.

Baddouh, A., Rguiti, M. M., El Ibrahim, B., Hussain, S., Errami, M., Tkach, V., Bazzi, L., & Hilali, M. (2019). Anodic oxidation of methylene blue dye from aqueous solution using SnO₂ electrode. *Iranian Journal of Chemistry and Chemical Engineering*, 38(5), 175-184.

Chang, S., Leu, I.-C., Liao, C., Yen, J.-H., & Hon, M.-H. (2004). Electrochemical behavior of nanocrystalline tin oxide electrodeposited on a Cu substrate for Li-ion batteries. *Journal of Materials Chemistry*, 14(12), 1821-1826.

Diya'uddeen, B. H., Daud, W. M. A. W., & Aziz, A. A. (2011). Treatment technologies for petroleum refinery effluents: A review. *Process Safety and Environmental Protection*, 89(2), 95-105.

El-Ghemy, A., Garcia-Segura, S., Rodríguez, R. M., Brillas, E., El Begrani, M. S., & Abdelouahid, B. A. (2012). Optimization of the electro-Fenton and solar photoelectro-Fenton treatments of sulfanilic acid solutions using a pre-pilot flow plant by response surface methodology. *Journal of Hazardous Materials*, 221, 288-297.

Fu, R., Zhang, P.-S., Jiang, Y.-X., Sun, L., & Sun, X.-H. (2023). Wastewater treatment by anodic oxidation in electrochemical advanced oxidation process: Advance in mechanism, direct and indirect oxidation detection methods. *Chemosphere*, 311, 136993.

Ghasempur, S., Torabi, S.-F., Ranaei-Siadat, S.-O., Jalali-Heravi, M., Ghaemi, N., & Khajeh, K. (2007). Optimization of peroxidase-catalyzed oxidative coupling process for phenol removal from wastewater using response surface methodology. *Environmental Science & Technology*, 41(20), 7073-7079.

Ho, N. A. D., Duong, H. L., Van Nhat, B., Dan, N. H., Thuan, N. C., Son, T. B., Hoinkis, J., & Le Luu, T. (2022). SnO₂-mixed oxide electrodes for water treatment: role of the low-cost active anode. In *Cost-efficient Wastewater Treatment Technologies: Engineered Systems* (pp. 255-284). Springer, Cham.

Hoang, N. T., Nguyen, X. C., Le, P.-C., Juzsakova, T., Chang, S. W., & Nguyen, D. D. (2021). Electrochemical degradation of pesticide Padan 95SP by boron-doped diamond electrodes: The role of operating parameters. *Journal of Environmental Chemical Engineering*, 9(3), 105205.

Husin, N. I., Wahab, N. A. A., Isa, N., & Boudville, R. (2011). Sorption equilibrium and kinetics of oil from aqueous solution using banana pseudostem fibers. 2011 *International Conference on Environment and Industrial Innovation*, IACSIT Press, Singapore.

Itoi, H., Takagi, K., Usami, T., Nagai, Y., Suzuki, H., Matsuoka, C., Iwata, H., & Ohzawa, Y. (2023). Electrochemical oxidation of anthracene to anthraquinone inside the nanopores of activated carbon: implications for electrochemical capacitors. *ACS Applied Nano Materials*, 6(13), 11541-11552.

Jawad, S. S., & Abbar, A. H. (2019). Treatment of petroleum refinery wastewater by electrochemical oxidation using graphite anodes. *Al-Qadisiyah Journal for Engineering Sciences*, 12(3), 144-150.

Jiad, M. M., & Abbar, A. H. (2023). Treatment of petroleum refinery wastewater by electrofenton process using a low cost porous graphite air-diffusion cathode with a novel design. *Chemical Engineering Research and Design*, 193, 207-221.

Jiad, M. M., & Abbar, A. H. (2024). Petroleum refinery wastewater treatment using a novel combined electro-Fenton and photocatalytic process. *Journal of Industrial and Engineering Chemistry*, 129, 634-655.

Jiang, Y., Zhao, H., Liang, J., Yue, L., Li, T., Luo, Y., Liu, Q., Lu, S., Asiri, A. M., & Gong, Z. (2021). Anodic oxidation for the degradation of organic pollutants: anode materials, operating conditions and mechanisms. A mini review. *Electrochemistry Communications*, 123, 106912.

Kalantary, R. R., Farzadkia, M., Kermani, M., & Rahmatinia, M. (2018). Heterogeneous electro-Fenton process by Nano-Fe₃O₄ for catalytic degradation of amoxicillin: Process optimization using response surface methodology. *Journal of Environmental Chemical Engineering*, 6(4), 4644-4652.

Khaleel, G. F., Ismail, I., & Abbar, A. H. (2023). Application of solar photo-electro-Fenton technology to petroleum refinery wastewater degradation: Optimization of operational parameters. *Heliyon*, 9(4), e15062.

Khataee, A., Vahid, B., Behjati, B., & Safarpour, M. (2013). Treatment of a dye solution using photoelectro-fenton process on the cathode containing carbon nanotubes under recirculation mode: Investigation of operational parameters and artificial neural network modeling. *Environmental Progress & Sustainable Energy*, 32(3), 557-563.

Khataee, A., Vahid, B., Behjati, B., Safarpour, M., & Joo, S. W. (2014). Kinetic modeling of a triarylmethane dye decolorization by photoelectro-Fenton process in a recirculating system: nonlinear regression analysis. *Chemical Engineering Research and Design*, 92(2), 362-367.

Kowal, A., Gojković, S. L., Lee, K.-S., Olszewski, P., & Sung, Y.-E. (2009). Synthesis, characterization and electrocatalytic activity for ethanol oxidation of carbon supported Pt, Pt-Rh, Pt-SnO₂ and Pt-Rh-SnO₂ nanoclusters. *Electrochemistry Communications*, 11(4), 724-727.

Liu, H.-L., & Chiou, Y.-R. (2005). Optimal decolorization efficiency of Reactive Red 239 by UV/TiO₂ photocatalytic process coupled with response surface methodology. *Chemical Engineering Journal*, 112(1-3), 173-179.

Machado, C. F., Gomes, M. A., Silva, R. S., Salazar-Banda, G. R., & Eguiluz, K. I. (2018). Time and calcination temperature influence on the electrocatalytic efficiency of Ti/SnO₂: Sb (5%), Gd (2%) electrodes towards the electrochemical oxidation of naphthalene. *Journal of Electroanalytical Chemistry*, 816, 232-241.

Mandal, P., Dubey, B. K., & Gupta, A. K. (2017). Review on landfill leachate treatment by electrochemical oxidation: Drawbacks, challenges and future scope. *Waste Management*, 69, 250-273.

Martínez-Huitl, C. A., & Brillas, E. (2009). Decontamination of wastewaters containing synthetic organic dyes by electrochemical methods: a general review. *Applied Catalysis B: Environmental*, 87(3-4), 105-145.

Martínez-Huitl, C. A., & Panizza, M. (2018). Electrochemical oxidation of organic pollutants for wastewater treatment. *Current Opinion in Electrochemistry*, 11, 62-71.

Molla Mahmoudi, M., Khaghani, R., Dargahi, A., & Monazami Tehrani, G. (2022). Electrochemical degradation of diazinon from aqueous media using graphite anode: effect of parameters, mineralisation, reaction kinetic, degradation pathway and optimisation using central composite design. *International Journal of Environmental Analytical Chemistry*, 102(8), 1709-1734.

Morales, U., Escudero, C. J., Rivero, M. J., Ortiz, I., Rocha, J. M., & Peralta-Hernández, J. M. (2018). Coupling of the electrochemical oxidation (EO-BDD)/photocatalysis (TiO₂-Fe-N) processes for degradation of acid blue BR dye. *Journal of Electroanalytical Chemistry*, 808, 180-188.

Mota, L. (2005). Development of a photochemistry reactor applicable in the treatment of phenolic wastewater present in the petroleum industry Master's Thesis, Rio Grande do Norte Federal University, Brazil. *Materials Science and Engineering*, 1076(2021), 012027.

Moussavi, G., Khosravi, R., & Farzadkia, M. (2011). Removal of petroleum hydrocarbons from contaminated groundwater using an electrocoagulation process: Batch and continuous experiments. *Desalination*, 278(1-3), 288-294.

Newell, R. G., Qian, Y., & Raimi, D. (2016). *Global energy outlook 2015*. National Bureau of Economic Research.

Peng, L., Liu, H., Wang, W.-L., Xu, Z.-B., Ni, X.-Y., Wu, Y.-H., Wu, Q.-Y., & Hu, H.-Y. (2020). Degradation of methylisothiazolinone biocide using a carbon fiber felt-based flow-through electrode system (FES) via anodic oxidation. *Chemical Engineering Journal*, 384, 123239.

Peralta-Hernández, J. M., de la Rosa-Juárez, C., Buzo-Muñoz, V., Paramo-Vargas, J., Cañizares-Cañizares, P., & Rodrigo-Rodrigo, M. A. (2016). Synergism between anodic oxidation with diamond anodes and heterogeneous catalytic photolysis for the treatment of pharmaceutical pollutants. *Sustainable Environment Research*, 26(2), 70-75.

Salman, R. H., & Abbar, A. H. (2023). Optimization of a combined electrocoagulation-electro-oxidation process for the treatment of Al-Basra Majnoon Oil field wastewater: Adopting a new strategy. *Chemical Engineering and Processing-Process Intensification*, 183, 109227.

Santos, I. D., Dezotti, M., & Dutra, A. J. (2013). Electrochemical treatment of effluents from petroleum industry using a Ti/RuO₂ anode. *Chemical Engineering Journal*, 226, 293-299.

Shao, D., Lyu, W., Cui, J., Zhang, X., Zhang, Y., Tan, G., & Yan, W. (2020). Polyaniline nanoparticles magnetically coated Ti/Sb-SnO₂ electrode as a flexible and efficient electrocatalyst for boosted electrooxidation of biorefractory wastewater. *Chemosphere*, 241, 125103.

Smith, A. (1998). Comparison of information-yield from different experimental designs used in algal toxicity testing of chemical mixtures. *Environmental Pollution*, 102(2-3), 205-212.

Stepnowski, P., Siedlecka, E., Behrend, P., & Jastorff, B. (2002). Enhanced photo-degradation of contaminants in petroleum refinery wastewater. *Water research*, 36(9), 2167-2172.

Sundaramoorthy, S., Singh, N., Taube, C. R., Katiyar, R., Muralidharan, V., & Palanivel, S. (2023). Electro-oxidation of tannery wastewater to achieve zero discharge—a step towards sustainability. *Environmental Technology*, 44(20), 2995-3003.

Yavuz, Y., Koparal, A. S., & Öğütveren, Ü. B. (2010). Treatment of petroleum refinery wastewater by electrochemical methods. *Desalination*, 258(1-3), 201-205.

Yu, F., Zhou, M., Zhou, L., & Peng, R. (2014). A novel electro-Fenton process with H₂O₂ generation in a rotating disk reactor for organic pollutant degradation. *Environmental Science & Technology Letters*, 1(7), 320-324.

Zhang, T., Liu, L., Qi, Q., Li, S., & Lu, G. (2009). Development of microstructure In/Pd-doped SnO₂ sensor for low-level CO detection. *Sensors and Actuators B: Chemical*, 139(2), 287-291.

Author(s) Information

Mohammed Hammid Jaeash

University of Al-Qadisiyah

Al-Qadisiyah, Iraq

Contact e-mail: mohammed.chemeng@qu.edu.iq

Husham M. Al-Tameemi

University of Al-Qadisiyah

Al-Qadisiyah, Iraq

To cite this article:

Jaeash, M.H. & Al-Tameemi, H.M. (2025). Treatment of petroleum refinery wastewater by electrooxidation using anode composed of composite materials. *The Eurasia Proceedings of Science, Technology, Engineering and Mathematics (EPSTEM)*, 37, 24-36.